Cytochrome *c*-Lipid Interactions: New Insights from Resonance Energy Transfer

Valeriya M. Trusova,[†△] Galyna P. Gorbenko,[†△] Julian G. Molotkovsky,[‡] and Paavo K. J. Kinnunen[§*]
[†]Department of Biological and Medical Physics, V. N. Karazin Kharkov National University, Kharkov, Ukraine; [‡]Shemyakin-Ovchinnikov Institute of Bioorganic Chemistry, Russian Academy of Sciences, Moscow, Russia; and [§]Helsinki Biophysics and Biomembrane Group, Institute of Biomedicine, University of Helsinki, Helsinki, Finland

ABSTRACT Resonance energy transfer (RET) from anthrylvinyl-labeled phosphatidylcholine (AV-PC) or cardiolipin (AV-CL) to cytochrome *c* (cyt *c*) heme moiety was employed to assess the molecular-level details of protein interactions with lipid bilayers composed of PC with 2.5 (CL2.5), 5 (CL5), 10 (CL10), or 20 (CL20) mol % CL under conditions of varying ionic strength and lipid/protein molar ratio. Monte Carlo analysis of multiple data sets revealed a subtle interplay between 1), exchange of the neutral and acidic lipid in the protein-lipid interaction zone; 2), CL transition into the extended conformation; and 3), formation of the hexagonal phase. The switch between these states was found to be controlled by CL content and salt concentration. At ionic strengths $\geq$40 mM, lipid bilayers with CL fraction not exceeding 5 mol % exhibited the tendency to transform from lamellar to hexagonal phase upon cyt *c* adsorption, whereas at higher contents of CL, transition into the extended conformation seems to become thermodynamically favorable. At lower ionic strengths, deviations from homogeneous lipid distributions were observed only for model membranes containing 2.5 mol % CL, suggesting the existence of a certain surface potential critical for assembly of lipid lateral domains in protein-lipid systems that may subsequently undergo morphological transformations depending on ambient conditions. These characteristics of cyt *c*-CL interaction are of great interest, not only from the viewpoint of regulating cyt *c* electron transfer and apoptotic propensities, but also to elucidate the general mechanisms by which membrane functional activities can be modulated by protein-lipid interactions.

INTRODUCTION

Cytochrome *c* (cyt *c*) is a small, highly basic hemoprotein abundantly found in the intermembrane space of mitochondria and possessing two biological functions that are, at first glance, unrelated. First, cyt *c* is strongly involved in respiration by shuttling the electrons from cyt *c* reductase (*bc*1 complex) to cyt *c* oxidase (1,2). The second mission of cyt *c* is related to the key role of this protein in activating the apoptotic pathway through cyt *c* release from mitochondria into the cytosol (3). It is generally established that binding to the inner membrane of mitochondria (IMM) ensures the realization of both protein functions. Despite the diversity of lipids constituting the mitochondrial membrane, leading part in cyt *c*-membrane binding belongs to cardiolipin (CL), a predominant component of IMM that is indispensable for protein retention, stability, and normal functioning (4). In view of this, the nature and specificity of interactions between cyt *c* and CL have remained for a long time a subject of extensive research (4–10). Despite some contradictions in molecular-level details, a consensus has been achieved regarding the general picture of cyt *c*-lipid complexation, postulating the existence of two distinct acidic phospholipid binding sites on the protein surface called the A- and C-sites (11–15). The A-site involves electrostatic interactions of deprotonated (DP) CL species with cyt *c*, whereas the C-site is stabilized by hydrogen bonding to protonated phosphate (HP) coupled with the formation of electrostatic contacts with deprotonated phosphate (16). Peculiar structural features of CL, together with the existence of a hydrophobic crevice in cyt *c* tertiary structure, led to the hypothesis of the so-called extended lipid conformation, in which lipid acyl chains point in opposite directions from the headgroup, producing a straight angle of 180° (14). In such an orientation, one acyl chain remains within the bilayer interior, whereas the other extends outward and is accommodated in the protein hydrophobic channel located near the heme crevice. Recently, it was hypothesized that this anchorage represents an abnormal conformation of cyt *c* that might facilitate its exit from mitochondria (15). In addition, it has been demonstrated that the changes in cyt *c* conformation upon its binding to the membranes include loosening of the protein tertiary structure, alterations in the heme environment, and loss of Met^{80}-iron ligation (1,9,15,17). However, the consequences of cyt *c*-CL interactions do not only include perturbation in protein conformation. A vast majority of studies indicate that association of this metalloprotein with the lipid matrix gives rise to modulation in composition and physical state of the annular layer of lipids (18,19). Specifically, cyt *c* was shown to induce changes in CL lateral distribution by ordering of the lipid molecules into microdomains and/or hexagonal (H_{II}) phases (18–20). This lipid sorting is predominantly electrostatic in origin and is dictated by

Submitted January 29, 2010, and accepted for publication June 7, 2010.

△Valeriya M. Trusova and Galyna P. Gorbenko contributed equally to this work.

*Correspondence: paavo.kinnunen@helsinki.fi

Editor: Thomas J. McIntosh.

© 2010 by the Biophysical Society

0006-3495/10/09/1754/10 $2.00

doi: 10.1016/j.bpj.2010.06.017

minimization of the electrostatic free energy of the protein-lipid system (19). It is important to point out that a plethora of studies showed that such CL structuring has significant physiological implications. Accordingly, it was conjectured that H_{II} configuration is favorable for the release of cyt *c* and other proapoptotic factors, and that cyt *c* entrapment inside CL structures enhances the rate of electron transfer displayed by this protein (18,21). Furthermore, formation of CL domains may lead to amplification of the apoptotic signal, remodeling of mitochondrial cristae, and loss of mitochondrial function observed during apoptosis (22,23). This process is also hypothesized to play a crucial role in energy channeling and opening of the mitochondrial permeability transition pore, early events in programmed cell death (24). In addition, CL clusters can potentially serve as a proton sink in membranes, particularly when they are in close proximity to oxidative phosphorylation complexes, and can enhance ATP synthase function (25). Finally, elevated local concentrations of CL are required for targeting of an osmosensory transporter, ProP, and for microphase separation (26). The fact that CL-enriched areas are involved in a wide variety of physiological and pathological processes as a means of organizing cyt *c*, as well as other membrane proteins, and of modulating their functional activity, together with the finding that cyt *c* may per se act as an inducer of CL assembly, strongly emphasizes the need for further in-depth exploration of this process.

Notwithstanding the great progress achieved in the field of cyt *c*-CL biophysics, the factors that initiate and regulate the protein-induced lipid sequestration still remain largely obscure. To the best of our knowledge, only a few attempts have been made to interpret quantitatively the effect of lipid segregation. Moreover, a number of experimental and theoretical works suggest that cyt *c*-induced formation of lipid domains and of H_{II} configurations are interdependent processes: domains may represent the intermediate states of nonbilayer structures (18,27). However, the parameters controlling the domain-to-hexagonal phase transition have to be elucidated. In an attempt to solve the above problems, we focused our attention in this article on clarifying the molecular-level details of electrostatically driven domain assembly in the model systems containing cyt *c* and phosphatidylcholine/cardiolipin (PC/CL) lipid vesicles. More specifically, our objectives were 1), to explore the ability of cyt *c* to induce molecular sorting of lipids in model membranes using steady-state resonance energy transfer (RET) under conditions of varying liposome composition, surface electrostatic potential of a lipid bilayer, ionic strength, and lipid/protein molar ratio (L/P); 2), to develop a Monte Carlo (MC) simulation procedure for a quantitative description of protein-initiated alterations in membrane surface topography and structural characterization of lipid domains; and 3), to establish the driving forces and precise molecular mechanisms of lateral segregation of membrane components.

The results obtained allowed us to establish the correlation between cyt *c*-induced lipid demixing, formation of the H_{II} phase, and extended lipid anchorage, thereby emerging with an integral picture of multifarious cyt *c*-CL interactions.

MATERIALS AND METHODS

Materials

Bovine heart CL, horse heart cyt *c* (oxidized form), NaCl, HEPES, and EDTA were purchased from Sigma (St. Louis, MO). 1-palmitoyl-2-oleoyl-*sn*-glycero-3-phosphocholine was from Avanti Polar Lipids (Alabaster, AL). Fluorescent lipids, 1-acyl-2-(12-(9-anthryl)-11-trans-dodecenoyl)-*sn*-glycero-3-phosphocholine (AV-PC), and 1-acyl-2-(12-(9-anthryl)-11-*trans*-dodecanoyl)-*sn*-glycero-3-phospho-1-rac-cardiolipin (AV-CL) were synthesized as described in detail elsewhere (28,29). All other chemicals were of analytical grade and used without further purification.

Preparation of lipid vesicles

Large unilamellar vesicles were made by extrusion technique from PC mixtures with 2.5, 5, 10, and 20 mol % CL (30). Appropriate amounts of lipid stock solutions were mixed in chloroform, evaporated to dryness under a gentle nitrogen stream, and then left under reduced pressure for 1.5 h to remove any residual solvent. The dry lipid residues were subsequently hydrated with 20 mM HEPES, 0.1 mM EDTA, pH 7.4, at room temperature to yield lipid concentration of 1 mM. Thereafter, the sample was subjected to 15 passes through a polycarbonate filter with a pore size of 100 nm (Millipore, Bedford, MA), yielding liposomes of the desired composition. AV-PC or AV-CL (0.26 and 0.13 mol %, respectively, of the total lipid) were added to the mixture of PC and CL before solvent evaporation. The presence of the AV probe did not influence the apparent particle size controlled by dynamic light scattering. The concentration of fluorescent lipid was determined spectrophotometrically using the AV extinction coefficient $\varepsilon_{367} = 9 \times 10^3\ M^{-1}cm^{-1}$ (28). Hereafter, liposomes containing 2.5, 5, 10, or 20 mol % CL are referred to as CL2.5, CL5, CL10, or CL20, with the subscript denoting the type of energy donor (AV-PC or AV-CL). The data sets obtained at different ionic strength are referred to as CL2.5/I20 or CL5/I40, where the figure after slash stands for the salt concentration in mM.

Fluorescence measurements

Fluorescence measurements were performed at 25°C using quartz cuvettes with a path length of 10 mm and a spectrofluorimeter equipped with a magnetically stirred, thermostated cuvette holder (LS-50B, Perkin-Elmer, Beaconsfield, United Kingdom). AV-PC and AV-CL emission spectra were recorded with an excitation wavelength of 367 nm. Excitation and emission slit widths were set at 5 nm. RET experiments were conducted with either AV-PC or AV-CL as donors and the heme group of cyt *c* as acceptor. Fluorescence intensity measured in the presence of cyt *c* at the maximum of AV emission (434 nm) was corrected for reabsorption and inner filter effects using the following coefficients (31):

$$k = \frac{\left(1 - 10^{-A_o^{ex}}\right)\left(A_o^{ex} + A_a^{ex}\right)\left(1 - 10^{-A_o^{em}}\right)\left(A_o^{em} + A_a^{em}\right)}{\left(1 - 10^{-(A_o^{ex} + A_a^{ex})}\right)A_o^{ex}\left(1 - 10^{-(A_o^{em} + A_a^{em})}\right)A_o^{em}}, \quad (1)$$

where A_o^{ex} and A_o^{em} stand for donor absorbance at the excitation and emission wavelengths in the absence of acceptor, and A_a^{ex} and A_a^{em} represent acceptor absorbance at the excitation and emission wavelengths,

respectively. The efficiency of energy transfer was determined by measuring the decrease of AV fluorescence upon addition of cyt *c*:

$$E = 1 - \frac{Q_{DA}}{Q_D} = 1 - Q_r, \quad (2)$$

where Q_D and Q_{DA} are the donor quantum yields in the absence and presence, respectively, of acceptor, and Q_r is the relative quantum yield.

RESULTS

In pursuit of a comprehensive picture of lipid lateral phase separation evoked by extrinsic membrane proteins in general, and cyt *c* in particular, our experimental strategy was directed toward collecting multiple data sets. More specifically, the relative quantum yield (Q_r) of donor (AV-PC or AV-CL) was measured as a function of acceptor (cyt *c*) concentration with the experimental parameters varying as follows: CL content at 2.5, 5, 10, and 20 mol %; lipid concentration (*L*) at 20 and 50 μM; and ionic strength (*I*) at 20, 40, and 60 mM.

It should be noted that whereas the RET experiments were performed with a range of liposomes (CL2.5, CL5, CL10, and CL20) and two types of donors, due to the very large amount of data collected (around 100 curves), we will discuss only the representative curves.

Features of RET profiles depending on liposome composition and donor type

Fig. 1 represents a set of RET curves obtained for different donors (AV-PC or AV-CL) at various CL mole fractions. The following salient features of RET profiles are noteworthy:

Absence of a definite dependence of energy transfer efficiency on CL content, suggesting that cyt *c*-lipid complexes are stabilized not only by electrostatic forces but also, presumably, by hydrophobic interactions.

Marked enhancement of energy transfer from the anionic donor AV-CL compared to the zwitterionic AV-PC in CL2.5 model membranes (Fig. 1 *A*), a hallmark of accumulation of anionic lipids in the vicinity of bound protein.

Inverted S-shape of the RET curves in CL20 systems for both AV-PC and AV-CL donors, which cannot be explained by the lateral movement of lipids and is attributable to the changes in cyt *c* transverse location. More specifically, given that the increment of acceptor concentration at the initial points of titration was rather small (~0.02 μM), the sigmoidality of the experimental plots is most likely the result of superposition of two curves with different saturation levels that correspond to two populations of membrane-bound cyt

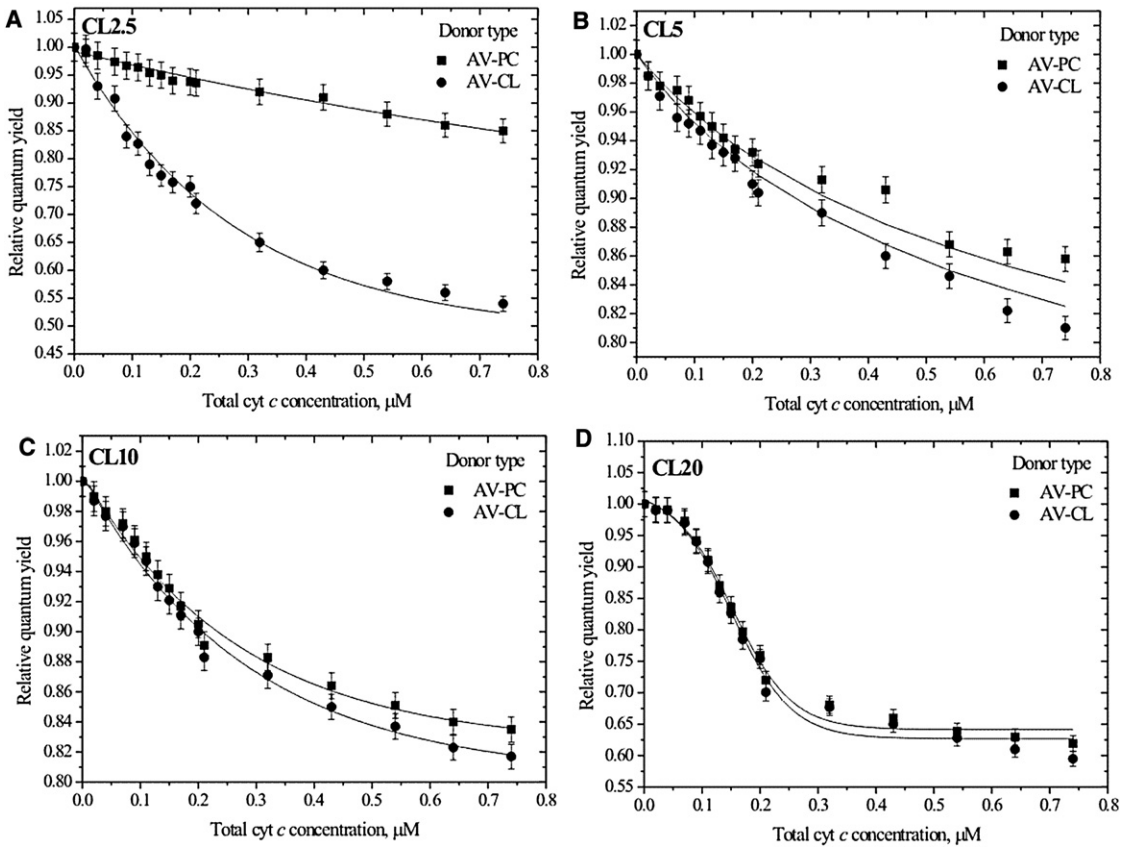

FIGURE 1 Comparison of AV-PC and AV-CL energy transfer profiles obtained for PC/CL liposomes containing 2.5 (*A*), 5 (*B*), 10 (*C*), or 20 (*D*) mol % CL under conditions of low ionic strength (20 mM). Lipid concentration was 20 μM. Solid lines are to guide the reader's eye.

c—surface-residing (where saturation level is reached at the third titration point) and bilayer-inserted (where saturation level coincides with that of the overall curve). Furthermore, the sigmoidal curves are characterized by an initial lag region (protein concentrations of ≤ 0.1 μM), which presumably reflects the protein accumulation at the lipid-water interface before approaching a certain critical surface coverage efficient to overcome the energy barrier for protein insertion into the membrane (32). It is interesting that the S-shaped dependency of RET efficiency on acceptor concentration was also observed by Bacalum and Radu in their investigation of energy transfer from Trp residues of the bacterial outer membrane porin to diphenylhexatriene, and the same conclusion was made about donor insertion (33).

Effect of lipid concentration on the behavior of RET curves

At the next stage of the study, we addressed the question of whether surface coverage could affect the RET profiles. It is evident from Fig. 2 that:

Decreasing lipid concentration is coupled with significant enhancement of RET, which can be explained by an increase in the surface concentration of the acceptor upon lowering the lipid concentration.

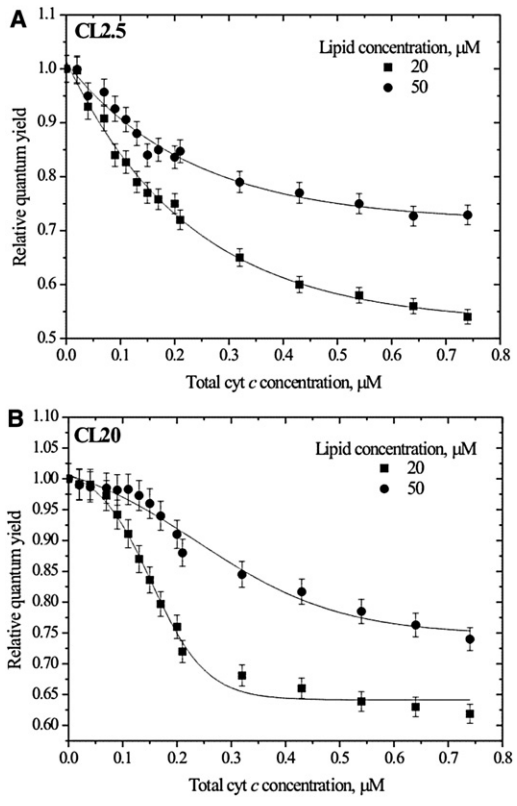

FIGURE 2 Effect of lipid concentration on RET in $CL_{AV\text{-}CL}$ model membranes: (*A*) 2.5 mol % CL, (*B*) 20 mol % CL. Ionic strength was 20 mM. Solid lines are to guide the reader's eye.

The lag period of sigmoidal RET curves observed for CL20 membranes depends on L (Fig. 2 *B*). For example, at $L = 20$ μM, the initial plateau ends at $P \approx 0.1$ μM, whereas at $L = 50$ μM this value is ~0.15 μM. Such behavior most likely arises from the different modes of cyt *c*-lipid binding depending on surface coverage or, in other words, on the L/P ratio. As hypothesized by Oellerich et al., at high L/P values, in excess of those of lipid, a lot of binding sites for the protein are available, and electrostatic association of cyt *c* with the membrane surface seems to be predominant (34). Lowering the L/P ratio increases the surface coverage and weakens the electrostatic forces due to the neutralization of the protein and membrane charges because of the formation of protein-lipid complexes. As a result, cyt *c* insertion into the hydrophobic part of the membrane effectively competes with peripheral, electrostatically controlled protein binding. Determining roughly that the completion of lag region is the beginning of protein embedment, the shift of the retardation phase toward higher P as lipid concentration is elevated indicates that at $L = 50$ μM, a cyt *c* concentration of 0.1 μM is insufficient for protein insertion to start. An analogous mechanism may explain the conversion of $Q_f(P)$ dependencies from sigmoidal to hyperbolic upon decreasing CL content (Fig. 1). With CL20 lipid membranes within the same protein concentration range (from 0 to ~0.1 μM), where electrostatic interactions more efficiently compete with hydrophobic ones compared to CL2.5 due to higher membrane surface potential, the process of cyt *c* insertion into the bilayer seems to be slower and can be detected by RET. It is important to note that all of the above considerations require further verification and will be the subject of more detailed analysis. Since in this work our attention was concentrated mainly on lipid segregation induced by cyt *c*, as we analyzed the experimental data we ignored RET curve deviations from the typical hyperbolic shape for liposomes with 20 mol % CL.

AV-cyt *c* energy transfer at varying ionic strength

The last step of our study was aimed at exploring the impact of solvent conditions on energy transfer from the AV lipids to the heme moiety. Elevating ionic strength turned out to have anomalous consequences for cyt *c*-lipid association. Conceptually, a rise in monovalent ion concentration would attenuate electrostatic protein-lipid interactions, thereby resulting in an overall decrease of energy transfer efficiency. This was the case for AV-PC containing liposomes (Fig. 3 *A*), but not for those with AV-CL, where RET exhibited an unexpected enhancement with increasing ionic strength (Fig. 3 *B*). As

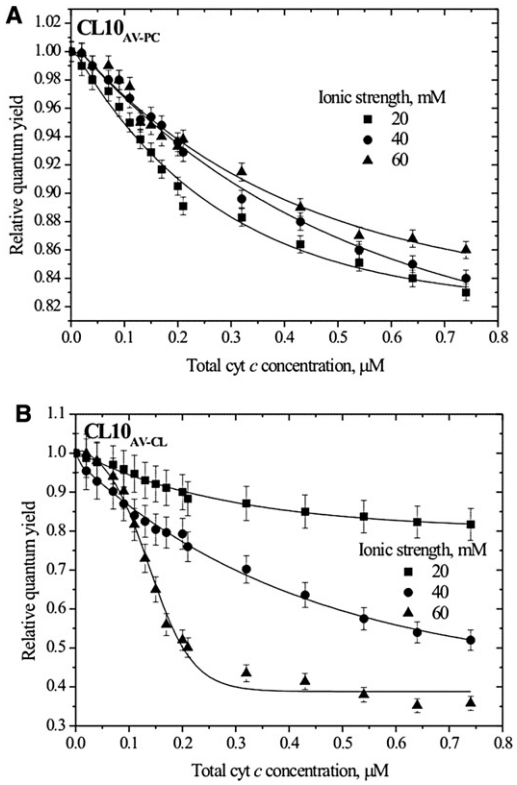

FIGURE 3 Relative quantum yield of AV-PC (*A*) and AV-CL (*B*) in PC/CL (10 mol %) liposomes under conditions of varying ionic strength. Lipid concentration is 20 μM. Solid lines are to guide the reader's eye.

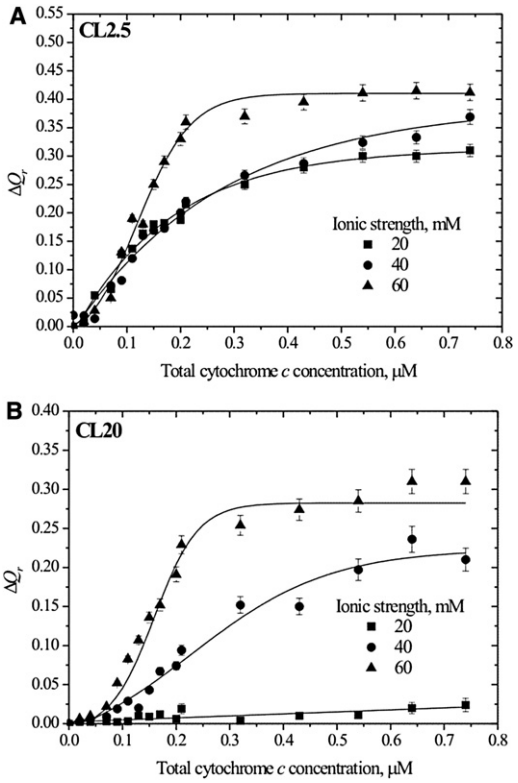

FIGURE 4 Difference between AV-PC and AV-CL relative quantum yields calculated as a function of total protein concentration for PC/CL model membranes containing 2.5 (*A*) or 20 (*B*) mol % CL. Lipid concentration is 20 μM. Solid lines are to guide the reader's eye.

a consequence, the difference between the relative quantum yields of AV-PC and AV-CL (ΔQ_r) did increase with ionic strength, this effect being most pronounced in weakly charged CL2.5 membranes (Fig. 4).

After briefly outlining the obtained results and highlighting the main findings, we now turn to quantitative data processing. As illustrated in Fig. 4 energy transfer from the anionic donor was much more pronounced than that from the zwitterionic donor, except for CL5, CL10, and CL20 vesicles at $I = 20$ mM, where RET curves obtained for either AV-PC or AV-CL as energy donors were virtually indistinguishable (data not shown for CL5 and CL10 systems). Among the possible reasons for this phenomenon, the most probable seems to involve local lipid demixing upon cyt *c* adsorption onto the surface of oppositely charged membranes, CL molecules moving toward the membrane-bound protein to minimize the electrostatic free energy of complexation. To account for this effect, and to extract the morphology of cyt *c*-induced lipid domains, we developed an MC simulation procedure the validity of which has been demonstrated in our previous study (20). In this algorithm, AV-CL donors were considered as randomly distributed within disk-shaped domains of radius r_{dm} centered at each acceptor's location. Our main goal was to determine characteristic domain size, i.e., dimensions of the protein-affected region where CL concentration is *k* times higher than that for a random lipid distribution. Overall, data treatment algorithm was based on three main steps: 1), determination of structural (heme distance from the bilayer center, *d*) and binding (intrinsic association constants, K_1^0 and K_2^0, and stoichiometry, *n*) characteristics of cyt *c*-lipid association within the framework of scaled-particle-theory-based adsorption and 2D RET models (see Supporting Material); 2), estimation of the concentration of bound protein (B_a); and 3), determination of domain size using MC simulation.

Optimization of the results obtained in terms of the combined RET-adsorption model revealed that the best-quality fit was achieved with the parameters presented in Table S1 in the Supporting Material. The recovered values of intrinsic constant were further used for evaluating the concentration of bound cyt *c* and calculating the number of donors and acceptors (Eqs. S26 and S28 in the Supporting Material) required for implementing the MC simulation. It should be noted that for $CL_{AV\text{-}PC}$ systems, the number of donors in domains, N_{AV-PC}^{dm}, proved to take on nonzero value ($N_{AV-PC}^{dm} = 1$) only at the highest surface densities of cyt *c*, thereby rendering RET profiles insensitive to variations in domain radius (r_{dm}) and the extent of CL segregation in the interaction zone (*k*). Therefore, the RET data obtained for $CL_{AV\text{-}PC}$ liposomes were treated using the MC approach, with d_1 and d_2 the only optimized parameters

(see Supporting Material). Next, the recovered d_1 and d_2 values were fixed and (r_{dm}, k) sets providing the best agreement between simulated and experimental data were derived from the MC analysis of $CL_{AV\text{-}CL}$ RET curves.

It should be noted that the basic MC algorithm turned out to be successful only in fitting the RET data obtained for the lowest ionic strength ($I = 20$ mM) (δ, the relative difference between experimental and theoretical Q_r values, did not exceed 2%). Remarkably, MC modeling of RET in CL2.5 systems at $I = 20$ mM demonstrated that the radius of CL-enriched zone upon varying k from 1 to 40 (the value corresponding to complete replacement of PC by CL) does not exceed 8.5 nm, highlighting the local pattern of cyt *c*-induced lipid lateral redistribution. On the contrary, in trying to fit the results of RET measurements acquired at ionic strengths of 40 and 60 mM using the basic MC procedure, we failed to achieve satisfactory agreement between theory and experiment (δ was >15%). This implies that the behavior of all other sets of RET measurements cannot be explained in terms of the simple assumption about lateral segregation of PC and CL upon cyt *c* binding. It is evident that the observed RET profiles reflect complex interplay between a number of interfering processes, which may involve lipid demixing, aggregation of interfacially adsorbed protein, and CL morphological changes (extended lipid conformation and nonbilayer structure).

DISCUSSION

Cyt *c*-CL interactions have been investigated with a variety of experimental techniques including SPR (35), atomic force microscopy (8,36), NMR (9), electron paramagnetic resonance (21), Fourier transform infrared spectroscopy (37), etc., and a wealth of data have been obtained to date. Of these methodologies, fluorescence techniques have superiority due to their extraordinary sensitivity, relative simplicity, high selectivity, and experimental convenience. Among different modifications of fluorescence spectroscopy, the utility and versatility of RET for examining the different facets of protein-lipid association, especially those concerning the resolution of spatial details of cyt *c*-CL complexes, are indubitable. In our previous study, we applied RET from AV-PC to the heme moiety of cyt *c* to extend the model of two distinct acidic phospholipid binding sites in the protein (A- and C-sites), with special attention to the effects of CL protonation (16). In this work, the use of two energy donors, AV-PC and AV-CL, allowed us to contribute further to the understanding of cyt *c*-CL biophysics by putting the examination of cyt *c* ability to control membrane morphology in the focus of our research. The observation that at $I = 20$ mM in CL5, CL10, and CL20 systems the efficiencies of energy transfer from neutral (AV-PC) and anionic (AV-CL) donors are identical suggest that in these types of lipid vesicles, cyt *c* exerts no influence on lipid lateral distribution. In contrast, in CL2.5 membranes, segregation-favoring screening of lipid charges by adsorbing cyt *c* molecules indicated strong lipid demixing. This finding is in line with the results of May et al., who showed that the most effective clustering of anionic lipids occurs for a weakly charged membrane and highly charged protein (38). It is important to note that the preferentially electrostatic nature of lipid domains and the small size of the AV fluorophore (~0.3 nm) relative to the length of lipid molecules provide strong grounds for believing that AV-PC and AV-CL resemble their nonlabeled counterparts in the way they partition into lipid domains.

As mentioned above, the radius of CL domains was found not to exceed 8.5 nm implicating molecular-scale deviation from the average lipid composition within and around the protein-membrane interaction zone (39–41). Higher ionic strengths seem to enhance the CL propensity to segregate, since the discrepancy between AV-PC and AV-CL RET profiles was present for all types of the model membranes investigated here. This phenomenon was explained by the assumption that along with protein binding, accumulation of monovalent ions near the bilayer surface may heavily contribute to membrane charge compensation. However, as shown by our results, the formation of regular planar CL domains is not the finite stage of cyt *c* association with all types of membranes at $I = 40$ mM and $I = 60$ mM, because a basic MC procedure, which accounts only for lipid demixing, turned out to be inapplicable for satisfactory fitting of experimental curves. Therefore, we scrutinized several hypotheses concerning the possible factors that could explain the observed enhancement of energy transfer at increasing salt concentrations.

Hypothesis I: imperfection of theoretical models

Extraction of quantitative information from RET data requires knowledge of the surface acceptor concentration (B_a). Here, this parameter was determined using a combined RET-adsorption model. The question arises whether the inherent imperfection of this model, associated with ignoring factors such as cyt *c* insertion into the lipid bilayer, protein conformational change, nonuniform charge distribution on the cyt *c* surface, etc., may influence the validity of the data analysis. To probe this question, we modeled two threshold situations—complete protein binding, i.e., $B_a = P$ (Fig. 5, *Case I*), and protein location in the bilayer center, i.e., $d_1 = 0$ and $d_2 = 0$ (Fig. 5, *Case II*). We considered only these cases, since mathematically increasing B_a and decreasing d yield Q_r reduction. However, as seen in Fig. 5, theoretical curves calculated by MC for these limiting cases still lie far above the experimental plot, suggesting that underestimation of B_a or overestimation of d cannot explain the discrepancy between simulation and experiment. Additional proof in favor of this viewpoint comes from the mimicking of cyt *c* adsorption behavior in terms of SPT and 2D RET models, which showed that if $B_a = P$, then d_1 and d_2 attain the

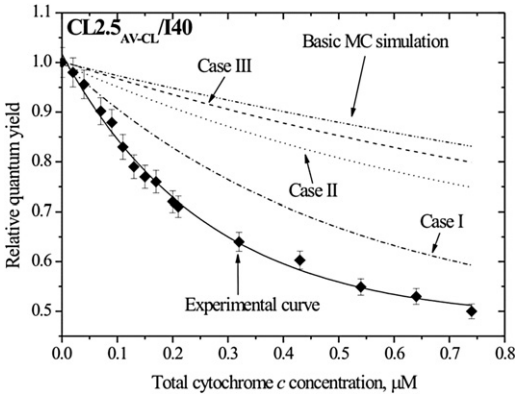

FIGURE 5 MC calculations of AV-CL relative quantum yield for the cases of the basic lipid demixing model (*dash-dot-dotted line*), the basic demixing model allowing for complete protein binding (*Case I*, *dash-dotted line*), cyt *c* location in the lipid bilayer center (*Case II*, *dotted line*), and aggregation of membrane-bound protein (*Case III*, *dashed line*). The experimental curve was obtained for PC/CL (2.5 mol % CL) liposomes at ionic strength 40 mM with donor AV-CL.

unrealistic magnitude of ~10 nm, whereas the maximum reasonable d value for our systems is ~4.5 nm.

Based on the above rationale, we concluded with a high degree of confidence that disagreement between experimental data and theoretical predictions is not a consequence of inherent uncertainties of the experimental and optimization procedures.

Hypothesis II: aggregation of membrane-bound cyt *c*.

A vast majority of studies demonstrate that association of cyt *c* with anionic lipids evokes protein conformational changes consistent with loosening of its tertiary structure and partial unfolding (42). The lipid bilayer can lower the activation energy barrier for protein unfolding, providing an environment with reduced pH and decreased dielectric constant, whose concerted action enhances side-chain charge repulsion, thereby giving rise to a more open structure with exposed aggregation-prone areas. According to our calculations, pH decrease compared to the bulk phase can be as large as 0.6, 0.9, 1.3, and 1.8 pH units for CL2.5, CL5, CL10, and CL20 vesicles, respectively. Furthermore, sophisticated theoretical analysis by Heimburg and Marsh coupled with elegant electron spin resonance experiments revealed that at ionic strengths >40 mM, surface-denaturated protein monomers exhibit a strengthened tendency for self-association (43). Assuming that lipid domains are formed around protein oligomers, the total number of domains can be defined as $N_{dm} = B_a N_A / z_p$, where z_p is the degree of protein oligomerization. However, as judged from Fig. 5 (*Case III*), this assumption didn't improve the data fitting, thereby invalidating this hypothesis. Indeed, if the demixing occurs locally, i.e., in the vicinity of singly adsorbed protein or peptide, there is no thermodynamical incentive for adsorbate aggregation (38).

Hypothesis III: transition of CL into the extended lipid conformation

As mentioned in the Introduction, cyt *c* binding to CL-containing membranes may result in adoption of lipid molecules of the extended conformation. This frustration is specific for CL and is dictated by the amphiphile tendency to minimize the bending stress created by high negative curvature. It was supposed that strong electrostatic interactions between a network of positively charged amino acid residues (Lys_{72}, Lys_{73}, and Lys_{86}) and DP cardiolipin in the case of the A-site, and H-bonds between Asn_{52} and the HP lipid in the case of the C-site, hold the acyl chain in the protein groove (12,15). If one assumes that CL adopts such a conformation and the acyl tail bearing the AV chromophore protrudes out of a membrane entering the hydrophobic cavity of cyt *c*, the enhancement of energy transfer might be expected due to the reduction in donor-acceptor separation distance. Indeed, allowing for this phenomenon in MC simulation by varying the zeta coordinate of donor and introducing the additional parameter D_{CE}, standing for the distance between bilayer center and the plane of donors adopting the extended conformation, had a partially beneficial effect and provided a satisfactory fit of experimental results for CL10 and CL20 liposomes. Approximation of the experimental data by the combined domain + extended lipid conformation MC model yielded radii of CL-enriched areas in the ranges 3.2–9.2 ($CL10_{AV\text{-}CL}$/I40), 2.5–6.2 ($CL20_{AV\text{-}CL}$/I40), 4.1–11.3 ($CL10_{AV\text{-}CL}$/I60), and 3.5–7 nm ($CL20_{AV\text{-}CL}$/I60), depending on k (Fig. 6). These estimates suggest that domain radius (taken at certain k) increases with ionic strength and decreases with CL content.

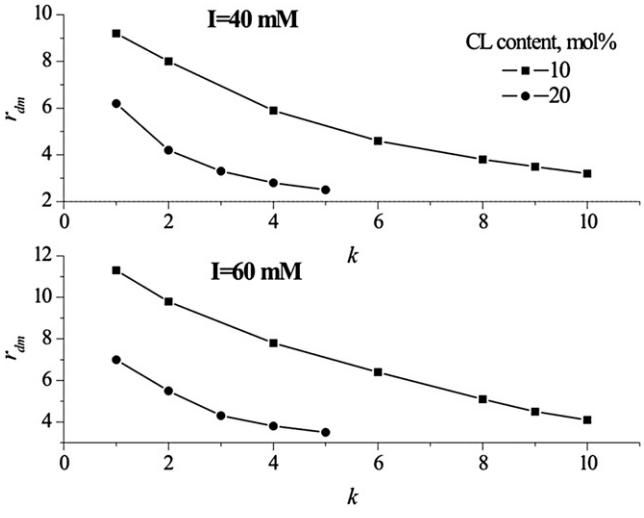

FIGURE 6 Membrane domain characteristics recovered from the combined lipid demixing + extended lipid anchorage MC model for CL10 (*squares*) and CL20 (*circles*) systems at ionic strength 40 (*upper*) and 60 mM (*lower*).

Yet, for $CL2.5_{AV\text{-}CL}$ and $CL5_{AV\text{-}CL}$ systems, the above data treatment strategy proved unsuccessful, suggesting the involvement of other factors.

Hypothesis IV: formation of nonbilayer structures

It follows from the above considerations that for CL10 and CL20 membranes, the unusual behavior of RET curves can be explained by reversal of the CL acyl chain with covalently bound AV into the cyt *c* crevice. Meanwhile, the question about the driving force of energy transfer amplification in CL2.5 and CL5 vesicles at increasing salt concentration remains open. Last, but not least, a putative mechanism that could provide an answer is the well-known ability of cyt *c* to trigger the formation of nonbilayer structures. In the early fundamental work by de Kruijff and Cullis, it was demonstrated that strong and specific cyt *c*-CL interactions may result in a hexagonal (H_{II}) lipid configuration (18). The authors postulated that the formation of protein-induced nonbilayer structures proceeds according to the pattern: adsorption of electrostatically governed protein onto the membrane surface → lipid demixing and formation of CL-enriched domains → local destabilization of the bilayer structure involving bilayer invagination → adoption of the lower-energy H_{II} phase. In keeping with this concept, we anticipated that gathering of CL molecules into domains, and their further transformation into regions with negative curvature, i.e., hexagonal cylinders around cyt *c*, would result in displacement of PC molecules from the protein vicinity and enhancement of RET. In distance terms, this scenario means that the minimal donor-acceptor separation in such a configuration is $R_{min} = R_P + D_m \approx 4.4$ nm, where R_P (2.1 nm) and D_m (2.3 nm) stand for protein radius and membrane halfwidth, respectively. According to the fundamental energy transfer law, it is evident that for the H_{II} phase, relative quantum yield can be as low as $Q_r = 1 - 1/[(\frac{R_{min}}{R_0})^6 + 1] \approx 0.4$, where $R_0 \approx 4.7$ nm is the Förster radius (the calculation of R_0 is given in the Supporting Material). The most pronounced energy transfer was observed for $CL2.5_{AV\text{-}CL}$/I60 liposomes with the value $Q_r = 0.44$ at the highest protein concentration lending support to the idea that the formation of nonbilayer structures can represent the main pathway, consistent with anomalous Q_r decrease in $CL2.5_{AV\text{-}CL}$ and $CL5_{AV\text{-}CL}$ membranes upon increasing *I*.

Armed with knowledge about the mechanisms occurring in our systems, we can now try to specify the ways by which salt concentration and CL content may control the switching between the regular CL-replete domains (CL2.5/I20), domains in which CL molecules adopt an additionally extended conformation (CL10/I40, CL20/I40, CL10/I60, and CL20/I60), and H_{II} structures (CL2.5/I40, CL5/I40, CL2.5/I60, and CL5/I60). A good deal of experimental and theoretical work has been invested in studies on lipid segregation induced by adsorption of oppositely charged cationic proteins (19,38–41,44). From these studies, a mechanism emerges according to which the fluid nature of the lipid bilayer allows the lipid constituent with the higher protein affinity to migrate laterally toward the interaction zone, modulating locally the lipid composition. If the curvature radius of anionic lipid-enriched areas exceeds that of the surrounding lipid, the membrane can further lower the interaction energy by bending and stretching, thereby changing the local curvature (44). Although elasticity of the membrane underlies the further possible structural transformations of the domains, initial crowding of specific lipids around the adsorbate is dictated by electrostatic protein-lipid interactions. However, as evidenced from our results, the formation of regular planar CL domains is not the finite stage of cyt *c* association with all types of membranes at $I = 40$ mM and $I = 60$ mM. Clustering of CL molecules creates gradients of curvature and line tension along the membrane surface. To compensate this energy cost, CL-enriched regions undergo structural transformations. In weakly charged vesicles, such reorganization manifests itself in the formation of the inverted hexagonal phase. In this geometry, electrostatic free energy reaches its minimum, because all lipid charges are in contact with protein charges, whereas in the lamellar phase only a fraction of anionic lipids are vicinal to cyt *c*. Several lines of evidence indicate that phospholipid polymorphism can be electrostatically controlled, and a number of anionic lipids may adopt the H_{II} configuration at low pH, or in the presence of high salt concentration or divalent metal cations (45). These observations are commonly explained by neutralization of anionic headgroup charges, which favors formation of the H_{II} over the lamellar phase. Apparently, on the one hand, elevating salt concentration enhances the demixing tendency of CL to such an extent that the most stable state for lipid domains would be a highly curved monolayer bent around the protein molecule. On the other hand, elevated ionic strength screens lipid charges, thereby strengthening the polymorphic potential of CL. In highly charged liposomes, conversion into the inverted hexagonal phase is somewhat hampered because of the high initial surface potential of the lipid bilayer. Moreover, due to the lower degree of demixing, transition into the hexagonal phase is not required for reaching a thermodynamic equilibrium, and the route by which the system further reduces the interaction energy seems to involve CL transition into the extended conformation. It is noteworthy, in this regard, that conditions facilitating the extended anchorage implicate increasing bilayer curvature and charge and decreasing headgroup size (15). These factors are believed to allow stronger electrostatic cyt *c*-lipid interactions, resulting in more pronounced conformational changes of both protein (greater extent of unfolding and wider opening of a crevice) and lipid that facilitate insertion of the acyl chain into the cyt *c* interior. It is clear that the above determinants readily

explain why CL protrudes into the protein only in the model membranes containing 10 and 20 mol % of anionic lipid—in the range of CL concentrations used here, the highest curvature and charge, and the smallest average headgroup size, are anticipated for CL10 and CL20 lipid bilayers. Meanwhile, the augmented ability of CL to adopt the extended conformation with increasing concentration of monovalent ions originates, apparently, from the alterations in polarity near the membrane surface. From a thermodynamic point of view, to insert into the protein, the lipid molecule should overcome the barrier associated with passage of the acyl chain through the highly polar bilayer surface. Increased salt concentration brings about a drop in the dielectric constant at the lipid-water interface and, as a consequence, reduction in interfacial polarity, which makes accommodation of the CL chain in the cyt *c* groove more energetically favorable.

CONCLUSIONS

Using resonance energy transfer and MC modeling we analyzed cumulatively the formation of CL-enriched areas induced by the adsorption of cyt *c* onto PC/CL membranes under varying experimental conditions. The key findings are as follows:

- At an ionic strength of 20 mM, cyt c triggers the formation of lipid domains in CL2.5 vesicles, with the radius of CL clusters not exceeding 8.5 nm.
- Higher ionic strength (>40 mM) enhances the CL demixing propensity and generates lateral heterogeneity in all types of model membranes investigated here.
- The size of lipid domains increases with ionic strength and reduction of CL content, pointing to a significant role of electrostatic effects in controlling membrane lateral organization.
- At ionic strengths of 40 and 60 mM in lipid bilayers containing 10 and 20 mol % CL, segregation of CL into lipid domains with high negative curvature is followed by CL transition into the extended conformation, tending to minimize the bending stress.
- For CL2.5 and CL5 membranes at ionic strengths of 40 and 60 mM, regular CL domains represent the intermediates in the transition from the lamellar to the hexagonal phase.

Our results may have important implications for a wealth of cellular activities, including fusion and fission of a membrane, cell sporulation and division, functioning of cyt *c* in mitochondria, the role of cyt *c* in apoptosis, and the overall biogenesis of the protein.

SUPPORTING MATERIAL

Twenty-eight equations and additional references are available at http://www.biophysj.org/biophysj/supplemental/S0006-3495(10)00728-9.

The authors are grateful to Drs. Yegor Domanov and Vladimir Zamotin for helpful discussions, and to Kristina Söderholm and Tiina Pasanen for their assistance.

This work was supported by grant No. 4534 from the Science and Technology Center in Ukraine, grant No. F28.4/007 from the Fundamental Research State Fund, and a grant from the European Social Fund (Project No. 2009/0205/1DP/1.1.1.2.0/09/APIA/VIAA/152). V.T. gratefully acknowledges an award from the Human Frontier Science Program. The Helsinki Biophysics and Biomembrane Group is supported by FP6 and FP7, The Finnish Academy, and the Sigrid Juselius Foundation.

REFERENCES

1. Pinheiro, T. J. T., H. Cheng, …, H. Roder. 2003. Direct evidence for the cooperative unfolding of cytochrome *c* in lipid membranes from H-^{2}H exchange kinetics. *J. Mol. Biol.* 303:617–626.
2. Shidoji, Y., K. Hayashi, …, K. Yagi. 1999. Loss of molecular interaction between cytochrome *c* and cardiolipin due to lipid peroxidation. *Biochem. Biophys. Res. Commun.* 264:343–347.
3. Schug, Z. T., and E. Gottlieb. 2009. Cardiolipin acts as a mitochondrial signalling platform to launch apoptosis. *Biochim. Biophys. Acta.* 1788:2022–2031.
4. Ostrander, D. B., G. C. Sparagna, …, W. Dowhan. 2001. Decreased cardiolipin synthesis corresponds with cytochrome *c* release in palmitate-induced cardiomyocyte apoptosis. *J. Biol. Chem.* 276:38061–38067.
5. Belikova, N. A., Y. A. Vladimirov, …, V. E. Kagan. 2006. Peroxidase activity and structural transitions of cytochrome *c* bound to cardiolipin-containing membranes. *Biochemistry.* 45:4998–5009.
6. Trusova, V. M., G. P. Gorbenko, …, A. Vasilev. 2009. A novel squarylium dye for monitoring oxidative processes in lipid membranes. *J. Fluoresc.* 19:1017–1023.
7. Bernad, S., S. Oellerich, …, S. Lecomte. 2004. Interaction of horse heart and *Thermus thermophilus* type *c* cytochromes with phospholipid vesicles and hydrophobic surfaces. *Biophys. J.* 86:3863–3872.
8. Choi, E. J., and E. K. Dimitriadis. 2004. Cytochrome *c* adsorption to supported, anionic lipid bilayers studied via atomic force microscopy. *Biophys. J.* 87:3234–3241.
9. Brown, L. R., and K. Wüthrich. 1977. NMR and ESR studies of the interactions of cytochrome *c* with mixed cardiolipin-phosphatidylcholine vesicles. *Biochim. Biophys. Acta.* 468:389–410.
10. Sinibaldi, F., L. Fiorucci, …, R. Santucci. 2008. Insights into cytochrome *c*-cardiolipin interaction. Role played by ionic strength. *Biochemistry.* 47:6928–6935.
11. Rytömaa, M., P. Mustonen, and P. K. J. Kinnunen. 1992. Reversible, nonionic, and pH-dependent association of cytochrome *c* with cardiolipin-phosphatidylcholine liposomes. *J. Biol. Chem.* 267:22243–22248.
12. Rytömaa, M., and P. K. J. Kinnunen. 1994. Evidence for two distinct acidic phospholipid-binding sites in cytochrome c. *J. Biol. Chem.* 269:1770–1774.
13. Rytömaa, M., and P. K. J. Kinnunen. 1995. Reversibility of the binding of cytochrome *c* to liposomes. Implications for lipid-protein interactions. *J. Biol. Chem.* 270:3197–3202.
14. Tuominen, E. K. J., C. J. A. Wallace, and P. K. J. Kinnunen. 2002. Phospholipid-cytochrome *c* interaction: evidence for the extended lipid anchorage. *J. Biol. Chem.* 277:8822–8826.
15. Kalanxhi, E., and C. J. A. Wallace. 2007. Cytochrome *c* impaled: investigation of the extended lipid anchorage of a soluble protein to mitochondrial membrane models. *Biochem. J.* 407:179–187.
16. Gorbenko, G. P., J. G. Molotkovsky, and P. K. J. Kinnunen. 2006. Cytochrome *c* interaction with cardiolipin/phosphatidylcholine model membranes: effect of cardiolipin protonation. *Biophys. J.* 90:4093–4103.
17. Nantes, I. L., M. R. Zucchi, …, A. Faljoni-Alario. 2001. Effect of heme iron valence state on the conformation of cytochrome *c* and its

association with membrane interfaces. A CD and EPR investigation. *J. Biol. Chem.* 276:153–158.

18. de Kruijff, B., and P. R. Cullis. 1980. Cytochrome *c* specifically induces non-bilayer structures in cardiolipin-containing model membranes. *Biochim. Biophys. Acta.* 602:477–490.
19. Heimburg, T., B. Angerstein, and D. Marsh. 1999. Binding of peripheral proteins to mixed lipid membranes: effect of lipid demixing upon binding. *Biophys. J.* 76:2575–2586.
20. Gorbenko, G. P., V. M. Trusova, …, P. K. Kinnunen. 2009. Cytochrome *c* induces lipid demixing in weakly charged phosphatidylcholine/phosphatidylglycerol model membranes as evidenced by resonance energy transfer. *Biochim. Biophys. Acta.* 1788:1358–1365.
21. Kagan, V. E., Y. Y. Tyurina, …, J. Jiang. 2006. The "pro-apoptotic genies" get out of mitochondria: oxidative lipidomics and redox activity of cytochrome *c*/cardiolipin complexes. *Chem. Biol. Interact.* 163:15–28.
22. Gonzalvez, F., and E. Gottlieb. 2007. Cardiolipin: setting the beat of apoptosis. *Apoptosis.* 12:877–885.
23. Ott, M., B. Zhivotovsky, and S. Orrenius. 2007. Role of cardiolipin in cytochrome *c* release from mitochondria. *Cell Death Differ.* 14:1243–1247.
24. Piccotti, L., M. Buratta, …, L. Corazzi. 2004. Binding and release of cytochrome *c* in brain mitochondria is influenced by membrane potential and hydrophobic interactions with cardiolipin. *J. Membr. Biol.* 198:43–53.
25. Mileykovskaya, E., and W. Dowhan. 2009. Cardiolipin membrane domains in prokaryotes and eukaryotes. *Biochim. Biophys. Acta.* 1788:2084–2091.
26. Epand, R. M., and R. F. Epand. 2009. Lipid domains in bacterial membranes and the action of antimicrobial agents. *Biochim. Biophys. Acta.* 1788:289–294.
27. Lipowsky, R., and R. Dimova. 2003. Domains in membranes and vesicles. *J. Phys. Condens. Matter.* 15:S31–S45.
28. Bergelson, L. D., J. G. Molotkovsky, and Y. M. Manevich. 1985. Lipid-specific fluorescent probes in studies of biological membranes. *Chem. Phys. Lipids.* 37:165–195.
29. Molotkovsky, J., M. Smirnova, M. Karyukhina, and L. Bergelson. 1989. Synthesis of anthrylvinyl phospholipid probes. *Bioorg. Khim. (Moscow).* 15:377–380.
30. Mui, B., L. Chow, and M. J. Hope. 2003. Extrusion technique to generate liposomes of defined size. *Methods Enzymol.* 367:3–14.
31. Bulychev, A. A., V. N. Verchoturov, and B. A. Gulaev. 1988. Current Methods of Biophysical Studies. Vyschaya Shkola, Moscow.
32. Zuckermann, M. J., and T. Heimburg. 2001. Insertion and pore formation driven by adsorption of proteins onto lipid bilayer membrane-water interfaces. *Biophys. J.* 81:2458–2472.
33. Bacalum, M., and M. Radu. 2007. Insertion of proteins in the lipid bilayer of liposomes revealed by FRET. *Romanian J. Biophys.* 17:129–138.
34. Oellerich, S., S. Lecomte, …, P. Hildebrandt. 2004. Peripheral and integral binding of cytochrome *c* to phospholipids vesicles. *J. Phys. Chem.* 108:3871–3878.
35. Salamon, Z., and G. Tollin. 1996. Surface plasmon resonance studies of complex formation between cytochrome *c* and bovine cytochrome *c* oxidase incorporated into a supported planar lipid bilayer. I. Binding of cytochrome *c* to cardiolipin/phosphatidylcholine membranes in the absence of oxidase. *Biophys. J.* 71:848–857.
36. Domènech, O., F. Sanz, …, J. Hernández-Borrell. 2006. Thermodynamic and structural study of the main phospholipid components comprising the mitochondrial inner membrane. *Biochim. Biophys. Acta.* 1758:213–221.
37. Choi, S., and J. M. Swanson. 1995. Interaction of cytochrome *c* with cardiolipin: an infrared spectroscopic study. *Biophys. Chem.* 54: 271–278.
38. May, S., D. Harries, and A. Ben-Shaul. 2000. Lipid demixing and protein-protein interactions in the adsorption of charged proteins on mixed membranes. *Biophys. J.* 79:1747–1760.
39. Binder, W. H., V. Barragan, and F. M. Menger. 2003. Domains and rafts in lipid membranes. *Angew. Chem. Int. Ed. Engl.* 42:5802–5827.
40. Mukherjee, S., and F. R. Maxfield. 2004. Membrane domains. *Annu. Rev. Cell Dev. Biol.* 20:839–866.
41. Mbamala, E. C., A. Ben-Shaul, and S. May. 2005. Domain formation induced by the adsorption of charged proteins on mixed lipid membranes. *Biophys. J.* 88:1702–1714.
42. Pinheiro, T. J. T., G. A. Elöve, …, H. Roder. 1997. Structural and kinetic description of cytochrome *c* unfolding induced by the interaction with lipid vesicles. *Biochemistry.* 36:13122–13132.
43. Heimburg, T., and D. Marsh. 1995. Protein surface-distribution and protein-protein interactions in the binding of peripheral proteins to charged lipid membranes. *Biophys. J.* 68:536–546.
44. Rinia, H. A., J. W. Boots, …, B. de Kruijff. 2002. Domain formation in phosphatidylcholine bilayers containing transmembrane peptides: specific effects of flanking residues. *Biochemistry.* 41:2814–2824.
45. Tarahovsky, Y. S., A. L. Arsenault, …, R. M. Epand. 2000. Electrostatic control of phospholipid polymorphism. *Biophys. J.* 79:3193–3200.